CNWRA *A center of excellence in earth sciences and engineering*

A Division of Southwest Research Institute®
6220 Culebra Road • San Antonio, Texas, U.S.A. 78228-5166
(210) 522-5160 • Fax (210) 522-5155

August 8, 2005
Contract No. NRC–02–02–012
Account No. 20.06002.01.332

U.S. Nuclear Regulatory Commission
Attn: Mr. Timothy J. Kobetz
Division of High-Level Waste Repository Safety
Two White Flint North
11545 Rockville Pike
Mail Stop 6-C11
Washington, DC 20555

Subject: Submission of Intermediate Milestone 20.06002.01.332.550: Assessment of Structural Robustness Against Aircraft Impact at the Potential Repository at Yucca Mountain—Progress Report

Dear Mr. Kobetz:

Attached is the Center for Nuclear Waste Regulatory Analyses document "Assessment of Structural Robustness Against Aircraft Impact at the Potential Repository at Yucca Mountain—Progress Report." This document fulfills the requirements for the subject milestone, which is due August 9, 2005.

This report summarizes progress made in developing staff capabilities to review and verify independently the U.S. Department of Energy assessments demonstrating robustness of certain structures of the proposed surface facilities at the potential geologic repository at Yucca Mountain, or portion thereof, to withstand certain aircraft crashes. Actual experimental observations of high explosive detonations and impact by simulated missiles on concrete walls were compared with analysis results using the finite element code LS-DYNA. As this report deals with selection of models appropriate for analyzing impact type problems, there are no safeguard restrictions. Actual simulations of aircraft impacting concrete structures will be conducted with safeguard restrictions imposed.

Washington Office • Twinbrook Metro Plaza #210
12300 Twinbrook Parkway • Rockville, Maryland 20852-1606

If you have any questions concerning this milestone, please contact me at 210.522.5151 or Amitava Ghosh at 210.522.3314.

Sincerely,

Asadul H. Chowdhury, Manager
Mining, Geotechnical, and
Facility Engineering

AHC: ar

cc:

B. Meehan	W. Patrick	Letter Only
D. DeMarco	B. Sagar	L. Gutierrez
E. Whitt	A. Chowdhury	CNWRA Directors
W. Reamer	A. Ghosh	CNWRA Element Mgrs
W. Ford	P. Cox	
T. McCartin	J. Mathis	
E. Collins	P. Maldonado	
L. Kokajko	Record Copy B, IQS	
K. Stablein		
M. Bailey		
J. Guttmann		

ASSESSMENT OF STRUCTURAL ROBUSTNESS AGAINST AIRCRAFT IMPACT AT THE POTENTIAL REPOSITORY AT YUCCA MOUNTAIN—PROGRESS REPORT

Prepared for

U.S. Nuclear Regulatory Commission
Contract NRC–02–02–012

Prepared by

P.A. Cox
J. Mathis
A. Ghosh

Center for Nuclear Waste Regulatory Analyses
San Antonio, Texas

August 2005

ABSTRACT

Hazards from crashes of aircraft flying in the vicinity of the proposed surface facilities at the potential repository at Yucca Mountain are a significant concern. The U.S. Department of Energy (DOE) has analyzed the expected annual frequency of aircraft crashes onto the surface facilities (Ragan, 2005). In this analysis, DOE has taken credit for the robustness of portions of the structures at different waste handling buildings and aging facility in reducing the estimated annual frequency of aircraft crashes. Staff has undertaken a study to develop capabilities to review and independently verify DOE assessments demonstrating structural robustness to withstand certain aircraft crashes. This report summarizes progress made in selecting appropriate material damage models for reinforced concrete under impact loads. Additionally, this report compares experimental observations of high explosive detonation and impact by simulated missiles on concrete walls with the numerical simulation results. As an outcome of the analysis carried out, the concrete damage model available in the finite element code LS-DYNA with appropriate erosion capabilities has been selected for modeling aircraft impacting a concrete structure. These analyses will be conducted in the future under appropriate imposed safeguard restrictions.

REFERENCE

Ragan, G.E. “Frequency Analysis of Aircraft Hazards for License Application.” 000–00C–WHS0–00200–000–00C. Las Vegas, Nevada: DOE, Office of Civilian Radioactive Waste Management. May 2005.

CONTENTS

Section Page

ABSTRACT . . . iii
FIGURES . . . vii
TABLES . . . ix
ACKNOWLEDGMENTS . . . xi

1 INTRODUCTION . . . 1-1
1.1 Background . . . 1-1
1.2 Objectives and Scope . . . 1-2

2 MATERIALS CHARACTERIZATION . . . 2-1
2.1 Reinforced Concrete Model for LS-DYNA . . . 2-1
2.2 Parameter Estimations . . . 2-2
2.2.1 Explosive Loading . . . 2-2
2.2.2 Impact Loading . . . 2-4
2.2.2.1 Small Scale Experiments . . . 2-5
2.2.2.2 Intermediate Scale Experiment . . . 2-11
2.2.2.3 Full Scale Experiment . . . 2-11
2.2.3 Summary of Parameter Estimation Analyses . . . 2-13

3 PRELIMINARY IMPACT STUDY OF A HYPOTHETICAL STRUCTURE . . . 3-1

4 SUMMARY AND CONCLUSIONS . . . 4-1

5 FUTURE WORK . . . 5-1

6 REFERENCES . . . 6-1

APPENDIX: DESCRIPTION OF LS-DYNA CONCRETE DAMAGE MATERIAL MODEL PARAMETERS

FIGURES

Figure Page

2-1 Simulation Setup for Explosive Detonation [1 ft = 0.3 mg 1 in = 2.5 cm] 2-3
2-2 Simulation Results of Velocity-Time Histories for Fragments of the Substantial Dividing Wall [1 ft/s = 0.3 m/s] 2-4
2-3 Concrete Equation of State Data Used in Numerical Simulation 2-8
2-4 Simulation of Small-Scale Missile Impacting the 12-cm [4.7-in] Thick Wall at 215 m/s [705 ft/s] Velocity Indicating Complete Perforation 2-8
2-5 Comparison of Measured Residual Velocities With Experimental Data 2-9
2-6 Velocity-Time History of the Missile Impacting 12 cm [4.7 in] Thick Wall 2-9
2-7 Simulation of Small-Scale Missile Impacting 12 cm [4.7 in] Thick Wall at 150 m/s [492 ft/s] Velocity Indicating Scabbing Damage at the Rear of the Wall 2-10
2-8 Simulation of Small-Scale Missile Impacting the 12 cm Thick Wall at 100 m/s [328 ft/s] Velocity Indicating Penetration at the Strike Face of the Wall 2-10
2-9 Simulation of Intermediate-Scale Missile Impacting the 35-cm [13.8-in] Thick Reinforced Wall at 215 m/s [708 ft/s] Velocity Indicating Complete Perforation of the Wall 2-12
2-10 Simulation of Intermediate-Scale Missile Impacting a 45 cm Thick Wall at 215 m/s [705 ft/s] Velocity. 2-12
2-11 Simulation of Intermediate-Scale Missile Impacting a 45 cm Thick Wall at 250 m/s [820 ft/s] Velocity. 2-13
2-12 Displacement Versus Time Comparison For Full-Scale Idealized Jet Engine Experiment 2-14
2-13 Crater on the Strike Face as Observed in the Simulation of Impact by a Full-Scale Idealized Jet Engine Missile 2-14

3-1 LS-DYNA Model of a Wall of a Hypothetical Structure 3-2
3-2 Force-Time History of Aircraft Impact 3-2
3-3 Displacement of the Wall Versus Time for an Impact of an F-16 at a Speed of 113 m/s [371 ft/s] 3-3
3-4 Contours of Stress on the Rear (Top) and Strike Face (Bottom) of the Wall in a Hypothetical Structure 3-3

TABLES

Table Page

2-1 Experiments Selected for Modeling 2-6
2-2 LS-DYNA Input Parameters for Concrete Model 2-7

ACKNOWLEDGMENTS

This report was prepared to document work performed by the Center for Nuclear Waste Regulatory Analyses (CNWRA) for the U.S. Nuclear Regulatory Commission (NRC) under Contract No. NRC–02–02–012. The activities reported here were performed on behalf of the NRC Office of Nuclear Material Safety and Safeguards, Division of High-Level Waste Repository Safety. The report is an independent product of CNWRA and does not necessarily reflect the views or regulatory position of NRC.

The authors would like to thank C. Weiss for the technical review, A. Chowdhury for the concurrence review, and S. Mohanty for the programmatic review of this report. The authors also appreciate A. Ramos for providing word processing support and E. Hanson for editorial support in preparation of this document.

QUALITY OF DATA, ANALYSES, AND CODE DEVELOPMENT

DATA: All CNWRA-generated original data contained in this report meet the quality assurance requirements described in the Quality Assurance Manual. Data used in this report are primarily experimental observations derived from other publicly available sources. Each data source is cited in this report and they should be consulted for determining the level of quality for those cited data.

ANALYSES AND CODES: The finite element analyses presented in this report were conducted using LS-DYNA, Version 970 (Livermore Software Technology Corporation, 2003). This version of the software is not under CNWRA configuration control. An earlier version of LS-DYNA software, Version 960, was validated and under CNWRA configuration control; but is not suited for parallel processing. The version of LS-DYNA that is appropriate for parallel computers (Version 970) has been used herein only for the development of capabilities. ANSYS LS-DYNA Version 9.0 will be used for safeguards analysis and validated after it is installed in the CNWRA stand-alone parallel computer system currently under procurement.

REFERENCE

Livermore Software Technology Corporation. “LS-DYNA User’s Manual.” Version 970. Livermore, California: Livermore Software Technology Corporation. April 2003.

1 INTRODUCTION

1.1 Background

A U.S. Nuclear Regulatory Commission (NRC) and U.S. Department of Energy (DOE) technical exchange and management meeting on preclosure safety analysis of the potential repository at Yucca Mountain was held in Las Vegas, Nevada, on July 24–26, 2001. Hazards from potential aircraft crashes onto the proposed surface facilities at the potential geologic repository operations area were discussed at this technical exchange. An agreement on aircraft crash hazards, PRE.03.01 (Reamer and Gil, 2001), was made between NRC and DOE after this meeting. This agreement asked for DOE to collect information on civilian and military aircraft flight activities in the vicinity of the Yucca Mountain site that may pose a hazard to the geologic repository operations area surface facilities. In addition, this agreement asked for DOE to perform analyses to estimate the annual frequency of aircraft crash hazard.

The DOE prepared two reports as a response to this agreement. These reports are (i) Identification of Aircraft Hazards (Morissette and Ziegler, 2002) and (ii) Frequency Analysis of Aircraft Hazards for License Application (Ragan, 2003). The NRC staff conducted a review of these reports and asked several clarifying questions to DOE (Schlueter, 2003a,b). The NRC and DOE staffs had another technical exchange on aircraft crash hazard on September 30, 2003, where DOE presented a summary of the two reports. Based on the discussion at this technical exchange, NRC decided to keep the agreement open. To address the concerns expressed by the NRC staff in Schlueter (2003a,b) and during the technical exchange on September 30, 2003, DOE revised the reports by Morissette and Ziegler (2002) and Ragan (2003) and developed two new reports: (i) Identification of Aircraft Hazards (Ashley, 2005) and (ii) Frequency Analysis of Aircraft Hazards for License Application (Ragan, 2005).

In this revised report by Ragan (2005), the following buildings, structures, and areas have been considered as having a potential for radiological release due to an aircraft crash: (i) Dry Transfer facilities, (ii) Canister Handling facility, (iii) Transportation Cask Buffer area, (iv) Transportation Cask Receipt/Return facility, (v) 1,000-MTHM aging pad, (vi) two 10,000-MTHM aging pads, (vii) two loaded waste-package or cask transporters, (viii) railcar buffer area, (ix) truck buffer area, (x) Fuel Handling facility, and (xi) low-level waste handling area. Additionally, DOE has changed the methodology used in Ragan (2003) to demonstrate that the annual frequency of aircraft crashing onto the surface facilities is a Beyond Category 2 event, (i.e., there is less than 1 in 10,000 chance of an accidental aircraft crashing onto the proposed geologic repository operations area surface facilities that may lead to a radiological release). DOE has taken credit for structural robustness of the exterior walls of the Dry Transfer facilities, Canister Handling facility, and Fuel Handling facility. These walls would be designed such that they would not be penetrated or collapsed by an F-16 aircraft crashing at the speed corresponding to the 95th percentile from a probability distribution estimated from historical F-16 crashes. Additionally, DOE has assumed that a barrier would be erected surrounding the aging pads to protect the aging casks against skidding aircraft (Ragan, 2005). It is believed that the barrier at least as tall as the aging casks and would be located on the fence line of the aging pads. This barrier would be designed to withstand penetration or collapse by an F-16 aircraft skidding onto it at the speed corresponding to the 95th percentile from a probability distribution of impact speed estimated from historical F-16 crashes. Furthermore, DOE has assumed that

the transportation casks with impact limiters are robust enough not to breach when impacted by a crashing aircraft.

10 CFR 63.112(e) requires that DOE should provide in the license application an analysis of the performance of the important to safety structures that are relied on to limit or prevent potential event sequences. DOE proposes to take credit for robustness of the walls of these facilities and the barrier wall of the aging facility to limit or prevent any event sequences initiated by a crashing aircraft with an impact speed corresponding to the 95th percentile of the probability distribution estimated from historical F–16 crashes only. DOE also proposes to submit calculations to substantiate the credit taken for structural robustness.

NRC and CNWRA staff will review DOE analyses in the license application on robustness of structures to withstand a potential aircraft crash and continue the safety functions assigned, thereby limiting or preventing potential event sequences. Additionally, staff should be able to independently verify DOE assessments of robustness of different structures.

1.2 Objectives and Scope

The ultimate objective of this study is to develop staff capabilities to review DOE analyses of structural robustness in the license application by independently modeling the phenomena associated with intense impact loading imparted by a crashing aircraft on reinforced concrete structures. This will allow staff to review and independently verify DOE assessments of specific structures to withstand aircraft crashes. Staff plan to conduct the impact analysis of a crashing aircraft under safeguard restrictions in a security room using a secured computer system with appropriate computing capabilities. The preparation of the security room and the procurement of the secured computer system are under progress. The computer code package that will be used for this analysis is ANSYS LS-DYNA Version 9.0 (Livermore Software Technology Corporation, 2005). While the secured computer system is being established, staff proceeded to address the adequacy of the modeling approach of the finite element computer code LS-DYNA (Livermore Software Technology Corporation, 2003) and the selection of parameters to characterize the response of reinforced concrete structures under intense impact loading up to and including failure. The study related to the adequacy of LS-DYNA modeling and selection of appropriate material models does not come under the purview of safeguard analysis. This nonsafeguard study deals with simulating the phenomena observed in experiments, with high explosive pressure pulse and simulated missiles striking a concrete wall. Comparing the numerical simulation results with the experimental observations helps to select the appropriate material damage models for concrete under impact loads in addition to establishing a methodology to determine the values for the model parameters. Additionally, a preliminary analysis has been conducted to experiment whether the selected material damage models can be used to simulate the impact of an aircraft on a wall. The load imparted by the aircraft has been simulated by an equivalent force-time history. Only local effects were simulated in this study so far. This report discusses the numerical simulations of the experiments and comparison with the experimental observations, including the analysis to simulate the impact of an aircraft. The selected material damage models will be used in the future as the continuation of the present study to simulate the impact of different types of aircraft on the waste handling buildings and the barrier of the aging facility of the geologic repository operations area surface facilities at the potential repository. These analyses may use characteristics of the actual structures under consideration and real threat (e.g., realistic models of the aircraft, realistic impact speed, etc.) and will be conducted in the future under safeguard restrictions.

2 MATERIALS CHARACTERIZATION

2.1 Reinforced Concrete Models for LS-DYNA

The modeling in this study was performed using the LS-DYNA Version 970 software developed by Livermore Software Technology Corporation (2003). LS-DYNA has several concrete material models built into the code, (e.g., the pseudo tensor model, soil/concrete model, Winfrith concrete model, and concrete damage model) (Livermore Software Technology Corporation, 2003). Each model has its specific applications and, in general, requires a different set of input parameters, some of which may not be easily obtainable from literature. For this analysis, the concrete damage model, which is essentially an improved version of the pseudo-tensor model, was selected.

The concrete damage model is a three-invariant plasticity model that accounts for changes in yield stress as a function of plastic strain using a damage function (Livermore Software Technology Corporation, 2003). A brief description of this model is given in the Appendix. A detailed description of the model is presented in Malvar, et al. (1997). This model was selected because it has been successfully used for modeling reinforced concrete structures where reinforcement bars are explicitly modeled as shared node beam elements (Livermore Software Technology Corporation, 2003). For this model, material parameters to represent concrete were calculated from known values of concrete compressive strength, using recommended procedures in both the LS-DYNA User's Manual (Livermore Software Technology Corporation, 2003) and Malvar, et al. (1997), as discussed in the Appendix of this report.

In addition to the material parameters for the concrete damage model, an equation of state is also needed to describe the pressure-compaction behavior of the concrete. The tabulated compaction model in the LS-DYNA manual was chosen, and values for the model were determined from a procedure found in the Winfrith concrete material model description in Livermore Software Technology Corporation (2003).

To complement the concrete model, a separate erosion algorithm was used to qualitatively model the break-up of the concrete material. The algorithm utilizes a limiting failure strain for the concrete. If the strain within an element reaches this limiting strain, the element will be deleted from the model in further calculations. As discussed in the Appendix, a parametric study was conducted to select a value for the strain at the failure of a concrete element. Along with a failure strain, a pressure erosion algorithm was investigated. This criterion is needed to limit the tensile pressure developed within an element. When the pressure limit is reached, the element is deleted from calculation, similar to the erosion failure strain criterion. This criterion was found to provide a good qualitative sense of the damage to the concrete, especially backside scabbing, as defined in Section 2.2.2, Impact Loading.

The reinforcement bars were modeled using beam elements, which shared nodes of the solid elements used for the concrete. The reinforcement bars were modeled using a kinematic elastic-plastic material model that allowed for yielding, strain hardening, and failure (Livermore Software Technology Corporation, 2003).

2.2 Parameter Estimation

In order to verify sensitivity and accuracy of input parameters describing the concrete model available in LS-DYNA Version 970, a comparison to available experimental observations was necessary. Two sources of experimental results were found in open literature and used for evaluating the concrete damage model. The first source of experimental results, as well as a good description of the concrete model used in LS-DYNA, was Malvar, et al. (1997). Malvar, et al. (1997) presented experiment results from an explosion against a substantial dividing wall and a comparison with numerical simulation results from the model. Substantial dividing walls are used to separate explosive materials in munition production and storage facilities. A second source of experimental results was Muto, et al. (1989a,b) and Esashi, et al. (1989). They provided results of impact experiments with both rigid and deformable missiles against reinforced concrete walls. The experimental program consisted of firing small and intermediate-scale idealized physical models of the GE J79 engine used in the F-4 Phantom fighter against scaled reinforced concrete walls. Full-scale experiments were also performed, and actual engines were used along with the full-scale idealized physical models (Muto, et al., 1989b).

Numerical simulations were performed using LS-DYNA (Livermore Software Technology Corporation, 2003) to reproduce the experiments described by Malvar, et al. (1997), Muto, et al. (1989a,b), and Esashi, et al. (1989). The purpose of these numerical simulations and correlations to experimental results was to demonstrate that LS-DYNA (Livermore Software Technology Corporation, 2003), with appropriate material models and parameters, can accurately predict the behavior of reinforced structures for intense blast and impact loading up to and including failure.

2.2.1 Explosive Loading

The verification set for explosive loading consists of modeling the detonation of a bomb containing 123 kg [272 lb] of high explosive inside a structure with substantial dividing walls, as presented in Malvar, et al. (1997). The substantial dividing wall is made of reinforced concrete with a thickness of 0.3 m [1 ft]. The concrete had #4 reinforcing bars at a spacing of 300 mm [12 in] in the horizontal and vertical directions on each side of the wall. A complete description of the experiment can be found in Malvar, et al. (1997).

Figure 2-1 shows the model created for the LS-DYNA analysis. Concrete material is modeled using six solid elements through the thickness, resulting in a 51-mm [2-in] cubical element size. The concrete compressive strength was not specified in Malvar, et al. (1997); a value of 241 MPa [3,500 psi] was assumed in this analysis, which exceeds the minimum requirements for substantial dividing walls. The reinforcing steel was modeled explicitly using beam elements. These elements shared nodes with the solid elements. The behavior of the reinforcing bars was modeled using the plastic-kinematic material model (Livermore Software Technology Corporation, 2003), with a yield stress of 496.4 MPa [72 ksi], an ultimate stress of 627.4 MPa [91 ksi], and a failure strain of 12 percent.

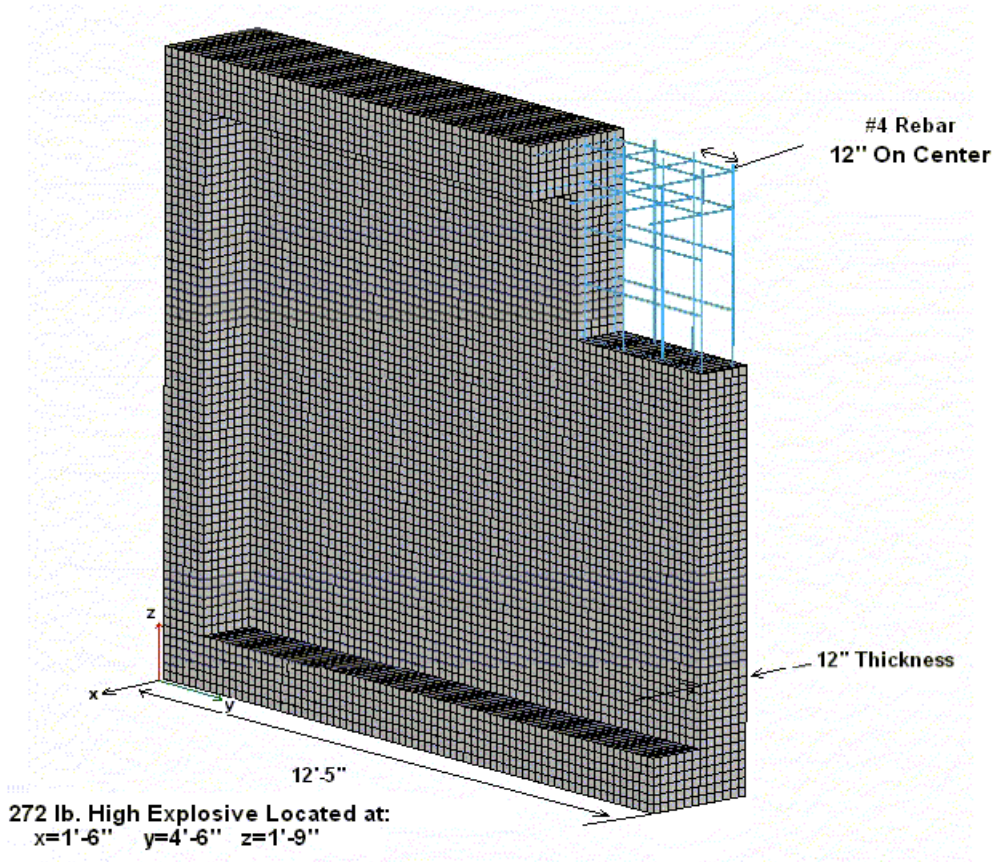

Figure 2-1. Simulation Setup for Explosive Detonation
[1 ft = 0.3 mg 1 in = 2.5 cm]

Loading is determined using the conventional weapons effects program (Hyde, 1992, 2004) algorithm available in LS-DYNA (Livermore Software Technology Corporation, 2003). Invoking this option in LS-DYNA automatically applies a transient pressure to element surfaces. The transient pressure is determined from the peak reflected pressure and reflected impulse provided by the conventional weapons effects program algorithm. To simulate loading on the wall, a surface burst is specified in the LS-DYNA model at the center of the mass of the bomb, as described in Malvar, et al. (1997). The case of the bomb is taken into account by using the Fano equation (Brit, et al., 2001), which calculates an effective charge weight considering the energy required for case break-up. This equation yielded an equivalent of a 110-kg [243-lb] trinitrotoluene charge. This equivalent explosive weight is also consistent with calculations using Blast-X (Brit, et al., 2001). The results of the experiment (Malvar, et al., 1997), showed velocities of the wall fragment to be on the order of 152.4 m/s [500 ft/s]. Results from the LS-DYNA numerical simulation, as illustrated in Figure 2-2, show that fragment velocities closely match the experiment results reported by Malvar, et al. (1997), except at the initial numerical simulation period and the results of the numerical simulation performed by Malvar, et al. (1997).

Differences in the two curves at the initial numerical simulation period most likely result from the different loading methods used and the erosion algorithm employed in the current numerical simulation. Results, (Figure 2-2) suggest that material parameters and the equation of state

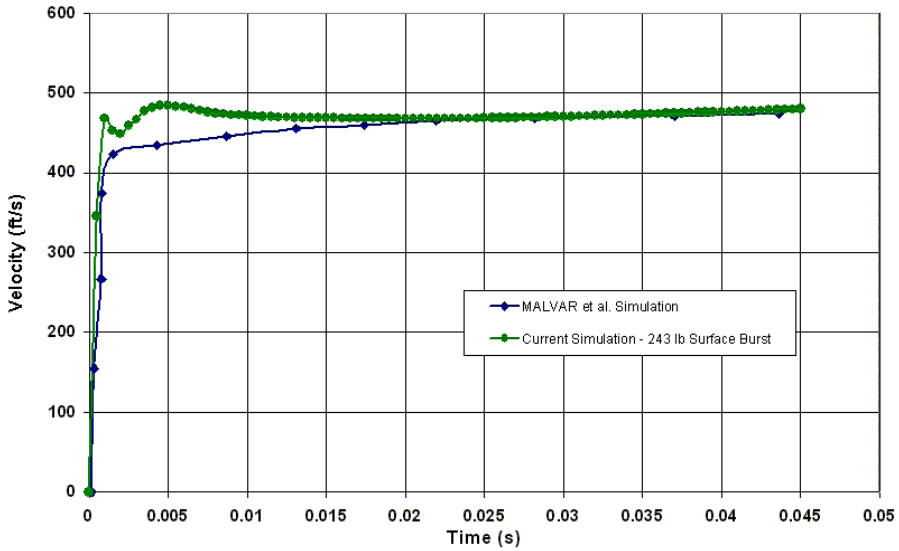

Figure 2-2. Simulation Results of Velocity-Time Histories for Fragments of the Substantial Dividing Wall [1 ft/s = 0.3 m/s]

values were appropriately selected in the current study and provide a good representation of the reinforced concrete walls response to blast loading.

2.2.2 Impact Loading

Numerical simulations of impact loading consisted of modeling the impact of deformable missiles made of steel, which represented simple models of jet engines, into reinforced concrete panels, as reported by Muto, et al. (1989a,b) and Esashi, et al. (1989). The missiles were idealized from the actual GE-J79 engine installed in the F-4 Phantom fighter aircraft (Muto, et al., 1989a). The missiles consisted of three concentrated masses connected by two thin cylindrical shells with the same stiffness and energy absorption capacity. Dimensions of the engine and the simplified models are given in Muto, et al. (1989a,b) and Esashi, et al. (1989).

The missiles used in these experiments hit targets of reinforced concrete walls with varying thicknesses that were supported at the corners with steel backup plates. Missile velocities were 100 m/s [328 ft/s], 150 m/s [492 ft/s], and 215 m/s [705 ft/s] for the small and intermediate scale experiments, and 215 m/s [705 ft/s] for the full-scale impact experiments. Experimental results were primarily descriptions of the damage produced by the impacts. Damage was classified by Muto, et al. (1989a) into four modes as follows:

(1) Perforation: Missile passed through target completely.

(2) Just Perforation: Missile does not pass through, but is stuck in the target. Perforation is just barely prevented, noted by breakage of reinforcement bars and a large opening.

(3) Scabbing: Considerable concrete debris is ejected off the back surface of the target, including a more severe case where a small opening is created on the rear surface.

(4) Penetration: A crater is formed on the front face of the target, but no damage occurs on the rear face.

Besides these four modes of damage observed and described, only limited instrumentation data were published (Muto, et al., 1989a,b; Esashi, et al., 1989). The only published data that facilitated a quantitative comparison between experimental and numerical simulation data were depth of penetration, a displacement time history for one experiment in the full-scale experiment series, and residual missile velocities for some of the small-scale experiments.

Selected small, intermediate, and full-scale impact experiments of Muto, et al. (1989a,b) and Esashi, et al. (1989) were chosen for modeling in LS-DYNA to further verify the concrete model behavior. Table 2-1 shows the selected experiments and the observed damage. These observed damage modes at the end of the experiment were compared with the corresponding LS-DYNA results presented in the next three subsections (2.2.2.1. 2.2.2.2, and 2.2.2.3).

2.2.2.1 Small Scale Experiments

The three small-scale experiments, conducted by Muto, et al. (1989a), were selected for numerical simulation in this study because three separate damage modes of the target wall were observed for the three impact velocities of the striking missile. The dimensions of the target wall were 1.5 m × 1.5 m × 12 cm [5 ft × 5 ft × 4.7 in]. The wall panel was supported at the four corners with steel backing plates. The concrete used to construct the wall had a measured compressive strength of 25.5 MPa [3.7 ksi]. Material properties for the concrete are listed in Table 2-2. A description of the parameters representing the material properties of concrete is given in Table 1 of the Appendix. Failure of the concrete was realized by a failure strain parameter used in the erosion algorithm of LS-DYNA (Livermore Software Technology Corporation, 2003). The reinforcement bars used to reinforce the concrete were 6-mm [0.24-in] diameter steel with 60 mm [2.4 in] center spacing in both directions and on both sides. The reinforcement bar yield strength was 447.2 MPa [65 ksi], with an ultimate strength of 585.1 MPa [85 ksi]. A failure strain of 12 percent was assumed for the plastic-kinematic material model of LS-DYNA (Livermore Software Technology Corporation, 2003). This is consistent with published material data for reinforcement bars (Wang and Salmon, 1998).

The missile used in the experiments was a 1/7.5 scale model of the GE-J79 engine installed in the F-4 Phantom fighter (Muto, et al., 1989a). The missile weight was 3.5 kg [7.7 lb], constructed with steel having a yield strength of 411.9 MPa [60 ksi] and ultimate strength of 705.1 MPa [102 ksi]. The missile was simulated with the plastic kinematic material model available in LS-DYNA (Livermore Software Technology Corporation, 2003).

The equation of state for concrete used in the numerical simulations is a tabulated function of pressure versus volumetric strain. Equation of state data can vary significantly for concretes with various strengths, ingredient mix ratios, and reinforcement ratios. As a result, a concrete compaction function was calculated from the suggested method documented in the Winfrith concrete model of LS-DYNA

Table 2-1. Experiments Selected for Modeling*†			
Wall Thickness (cm)	**Missile Weight (kg)**	**Missile Velocity (m/s)**	**Observed Damage Mode**
Small Scale (1/7.5 Scale GE-J79 Engine)			
12	3.5	215	Perforation
12	3.5	150	Scabbing
12	3.5	100	Penetration
Intermediate Scale (½.5 Scale GE-J79 Engine)			
35	100	215	Perforation
45	100	215	Scabbing
45	100	250	Just perforation
Full Scale			
160	1,463	215	Penetration

*Muto, K., H. Tachikawa, T. Sugano, H. Tsubota, H. Kobayashi, Y. Kasai, N. Koshika, and T. Tsujimoto. "Experimental Studies on Local Damage of Reinforced Concrete Structures by the Impact of Deformable Missiles, Part 1: Outline of the Test Program and Small-Scale Tests." Transaction of the 10th International Conference on Structural Mechanics in Reactor Technology (SMiRT 10). Los Angeles, California: American Association for Structural Mechanics in Nuclear Reactors. August 14–19, 1989a.

†Muto, K., H. Tachikawa, T. Sugano, H. Tsubota, N. Nagamatsu, N. Koshika, M. Okano, K. Suzuki, and S. Ohrui. "Experimental Studies on Local Damage of Reinforced Concrete Structures by the Impact of Deformable Missiles, Part 3: Full-Scale Tests." Transaction of the 10th International Conference on Structural Mechanics in Reactor Technology (SMiRT 10). Los Angeles, California: American Association for Structural Mechanics in Nuclear Reactors, August 14–19, 1989b.

(Livermore Software Technology Corporation, 2003). The equation of state used for the numerical simulation is shown in Figure 2-3.

Numerical simulation results for the 215 m/s [705 ft/s] impact (Figure 2-4) indicated a complete perforation of the wall, which agrees with the description of the damage observed in the experiment (Muto, et al., 1989a) as shown in Table 2-1 of this report. In addition to the qualitative observation of damage, the residual velocity of the missile after penetrating the wall was also recorded with high-speed cameras. Figure 2-5 shows measured residual velocity versus panel thickness using experimental results from Muto, et al. (1989a). Figure 2-6 shows a velocity-time history of the missile in the numerical simulation. The resultant residual velocity predicted in this numerical simulation at node 800119, located on the missile, shows good agreement with the measured residual velocity of approximately 55 m/s [180 ft/s] for the missile.

A second numerical simulation of missile impact at 150 m/s [492 m/s] also was performed. According to the experimental observations (Muto, et al., 1989a), the missile did not penetrate the wall completely; however, the wall suffered scabbing on the rear side. Figure 2-7 shows the results of this numerical simulation. Erosion of elements can be seen at rear face of the wall

Table 2-2. LS-DYNA Input Parameters for Concrete Model		
Material Parameters		
Variable	**Description**	**Value**
RO	Mass Density (kg/m^3)	2300
PR	Poisson's Ratio	0.19
SIGF	Maximum Principal Stress for Failure (Pa)	2.35×10^7
A0	Cohesion (Pa)	5.88×10^6
A1	Pressure Hardening Coefficient	0.333
A2	Pressure Hardening Coefficient	1.42×10^{-8}
A0Y	Cohesion for Yield (Pa)	2.64×10^6
A1Y	Pressure Hardening Coefficient for Yield Limit	0.745
A2Y	Pressure Hardening Coefficient for Yield Limit	3.10×10^{-8}
A1F	Pressure Hardening Coefficient for Failed Material	0.385
A2F	Pressure Hardening Coefficient for Failed Material	1.39×10^{-8}
B1	Damage Scaling Factor	1.250
B2	Damage Scaling Factor for Uniaxial Tensile Path	4.0
B3	Damage Scaling Factor for Triaxial Tensile Path	10.0

surface, indicating that scabbing has taken place. These results are consistent with the qualitative experimental observation presented in Muto, et al. (1989a).

A third numerical simulation of the missile impact was at a velocity of 100 m/s [328 ft/s]. At this velocity, experimental results show no scabbing, only a penetration into the strike surface of the wall. Numerical simulation results, as shown in Figure 2-8, are in agreement with the experimental observations. The strike face of the wall shows penetration, while no scabbing or element failure is apparent at the rear face.

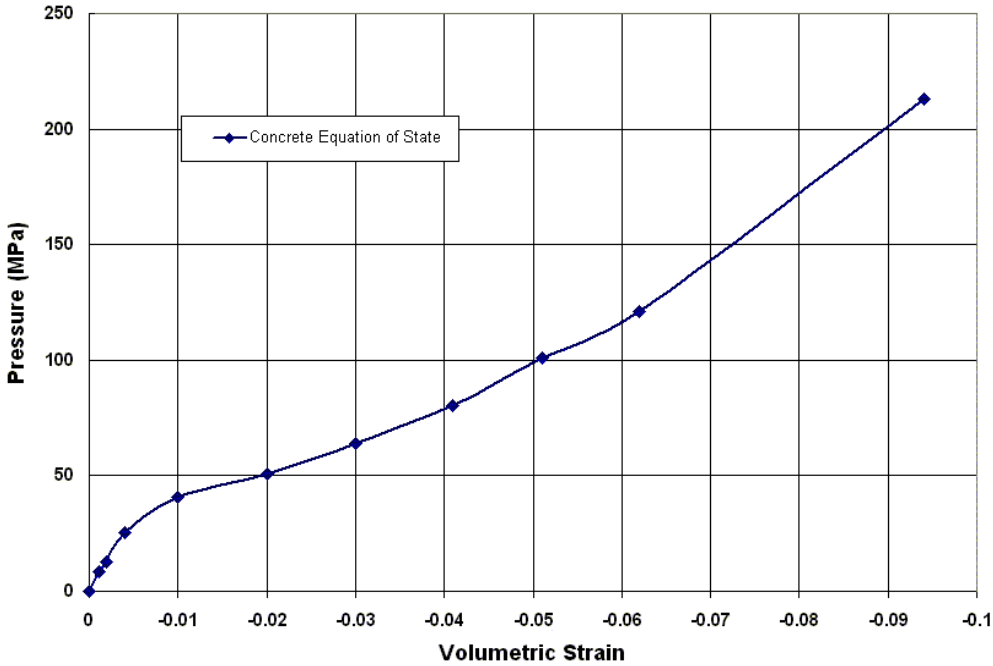

Figure 2-3. Concrete Equation of State Data Used in Numerical Simulation

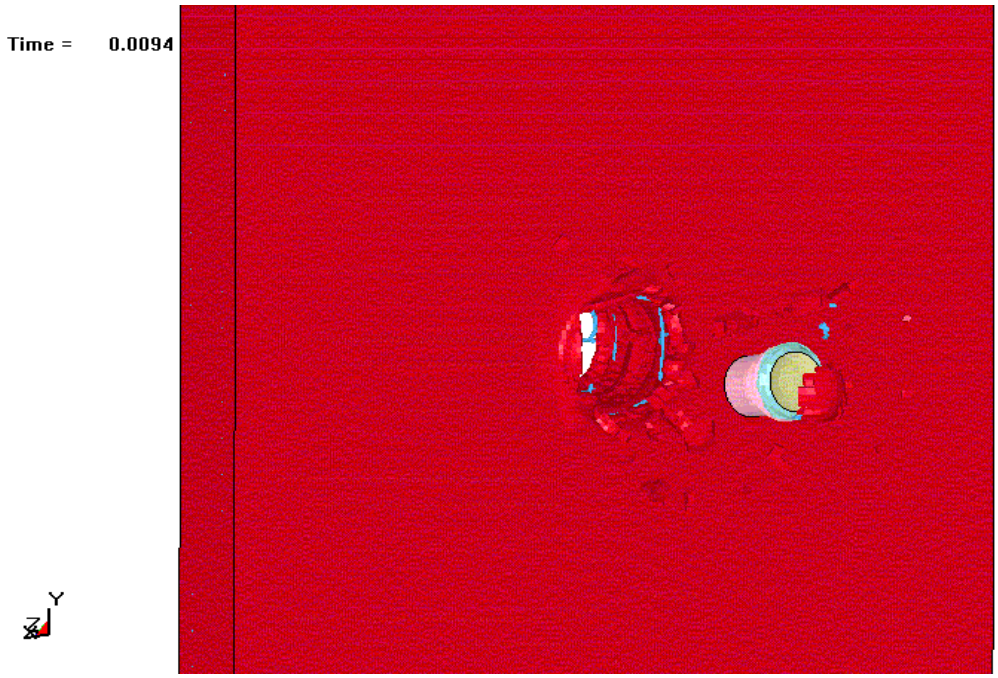

Figure 2-4. Simulation of Small-Scale Missile Impacting the 12-cm [4.7-in] Thick Wall at 215 m/s [705 ft/s] Velocity Indicating Complete Perforation

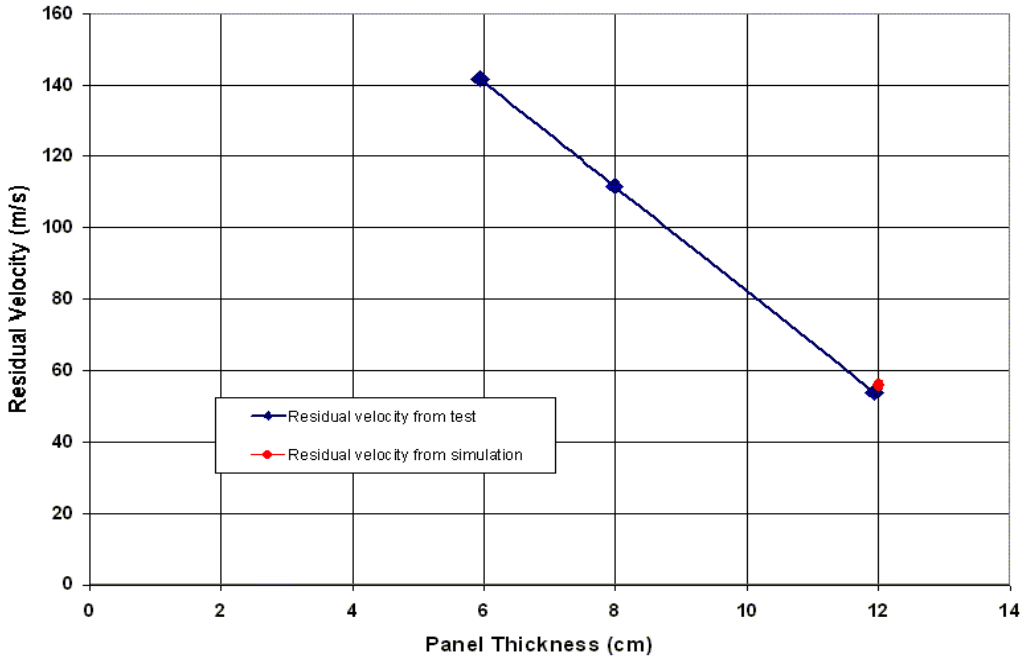

Figure 2-5. Comparison of Measured Residual Velocity With Experimental Data from Muto, et al. (1989a)

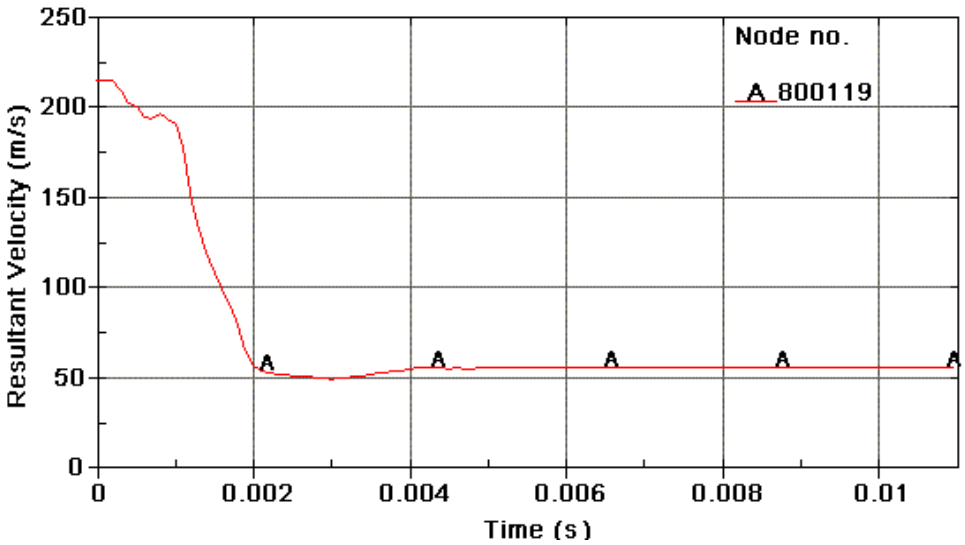

Figure 2-6. Velocity-Time History of the Missile Impacting 12-cm [4.7-in] Thick Wall

Figure 2-7. Simulation of Small-Scale Missile Impacting 12-cm [4.7-in] Thick Wall at 150 m/s [492 ft/s] Velocity Indicating Scabbing Damage at the Rear of the Wall.

Figure 2-8. Simulation of Small-Scale Missile Impacting the 12-cm [4.7-in] Thick Wall at 100 m/s [328 ft/s] Velocity Indicating Penetration at the Strike Face of the Wall. No Damage Observed at the Rear Face.

2.2.2.2 Intermediate Scale Experiment

Numerical simulations of the experiments, performed at a ½.5 intermediate scale by Esashi, et al. (1989), were also conducted in this study. The reinforced concrete walls used in the intermediate-scale experiments had a measured compressive strength of 32.3 MPa [4.7 ksi]. Based on this information, a new set of material model parameters was generated, along with a modification of the equation of state associated with the change in the concrete compressive strength, as explained in the Appendix. The reinforcement bars were spaced at 0.110 m [4.3 in] in both directions and on both sides. The bars had a diameter of 16 mm [0.63 in], yield strength of 360.6 MPa [55 ksi], and ultimate strength of 559.6 MPa [81 ksi]. Reinforcement bar strain at failure was assumed to be 12 percent. The missile was scaled by a factor ½.5 from the actual GE-J79 engine. The weight of the missile was 100 kg [220 lb] and was made of steel with a yield strength of 582.7 MPa [84.5 ksi] and an ultimate strength of 821.1 MPa [119 ksi].

The 35-cm [14-in] thick wall, impacted by the missile at a velocity of 215 m/s [705 ft/s], was simulated in LS-DYNA. Results from the experiment show complete perforation of the wall; however, no information on residual velocity is available. Figure 2-9 shows the numerical simulation results and indicates good agreement with the experiment.

Additionally, two numerical simulations of the missile impacting at velocities of 215 m/s [705 ft/s] and 250 m/s [782 ft/s] were conducted for a reinforced wall with a thickness of 45 cm [17.7 in]. Experimental results for this wall at an impact speed of 215 m/s [705 ft/s] indicated a scabbing mode of damage and significant penetration into the strike face. Figure 2-10 gives a close-up image of the numerical simulation results for both strike and rear faces of the wall. Significant penetration is evident on the strike face, and approximately 12 cm [4.7 in] displacement has been seen at the rear face. Scabbing is not apparent in this numerical simulation; however, the effectiveness of the wall to stop the missile and the overall damage of the wall are successfully simulated. The reinforcement bars at the rear face remained intact during the impact, which is consistent with the experimental observations.

The experiment with the missile impacting the 45 cm [17.7 in] thick wall at a speed of 250 m/s [820 ft/s] is a very good case to experiment the numerical simulation capability. Experimental results showed the missile lodged in the wall, but complete perforation did not take place. Results from the LS-DYNA numerical simulation are shown in Figure 2-11. Views of the strike face and back side of the experimental wall are given in this figure. The view of the strike face shows the missile at rest, lodged inside the wall, after approximately 350 ms. The rear side view shows significant material ejection along with reinforcement bar failure; however, complete perforation of the wall did not take place. Results from the numerical simulation are consistent with the overall damage observed in the experiment (Esashi, et al., 1989).

2.2.2.3 Full-Scale Experiment

A final comparison was made with the full-scale experiment using the idealized engine model reported in Muto, et al. (1989b). The full-scale reinforced concrete wall was a 7 m [23 ft] square, and had a thickness of 160 cm [63 in]. The measured concrete compressive strength was 23.5 MPa [3.4 ksi]. A total of 0.4 percent of reinforcement bars was used in each face, and in each direction. The reinforcement bar diameter was 32.3 mm [1.3 in] with a yield strength of 488.7 MPa [71 ksi] and an ultimate strength of 744.4 MPa [108 ksi]. An idealized engine with a total mass of 1,463 kg [3,225 lb] was used to impact the wall. The engine was 76 cm [30 in] in

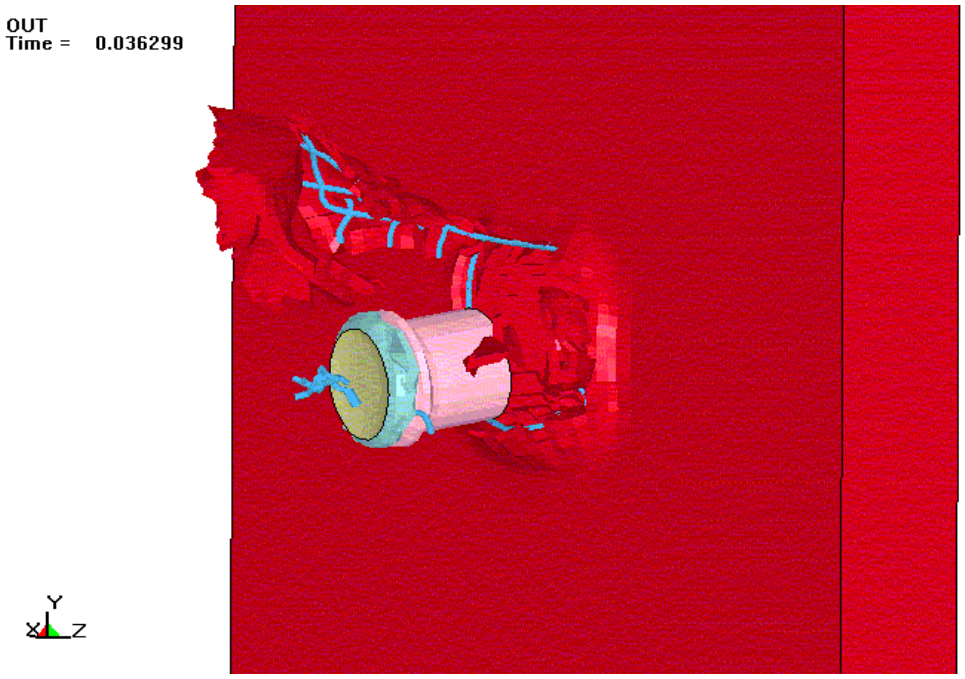

Figure 2-9. Simulation of Intermediate-Scale Missile Impacting the 35-cm [13.8-in] Thick Reinforced Wall at 215 m/s [705 ft/s] Velocity Indicating Complete Perforation of the Wall. Rear Face of the Wall Are Shown Here.

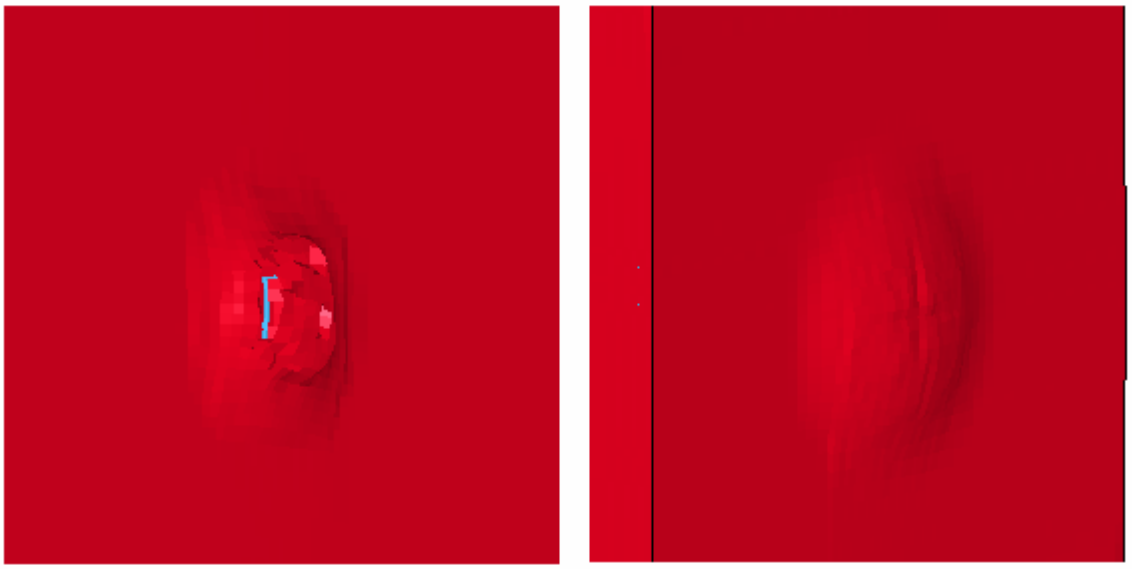

Figure 2-10. Simulation of Intermediate-Scale Missile Impacting a 45-cm [17.7-in] Thick Wall at 215 m/s [705 ft/s] Velocity. Both Strike (Left) and Rear (Right) Faces Are Shown Here Significant Penetration Occurred at the Strike Face.

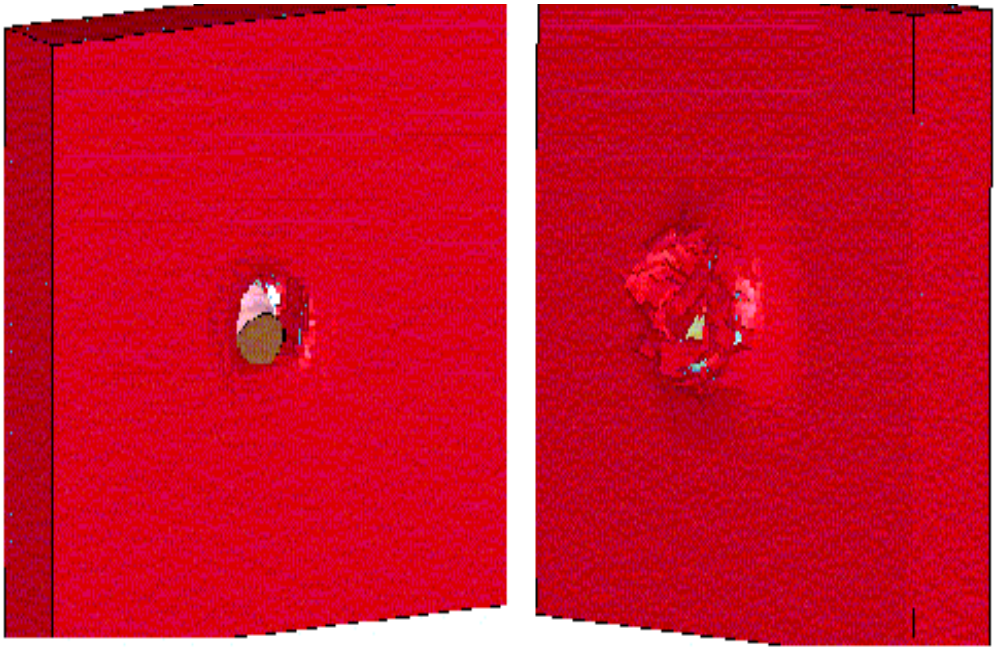

Figure 2-11. Simulation of Intermediate-Scale Missiles Impacting a 45-cm [17.7-in] Thick Wall at 250 m/s [820 ft/s] Velocity. Both Strike (Left) and Rear (Right) Faces Are Shown. Strike Face Shows the Lodged Missile. Complete Perforation is Not Observed at the Rear Side.

diameter and constructed of steel with a yield strength of 349.1 MPa [50.6 ksi] and an ultimate strength of 687.4 MPa [100 ksi].

Results of the experiment at an impact speed of 215 m/s [705 ft/s] showed penetration of about 21 cm [8.3 in] into the strike face of the wall, with no observed scabbing at the rear face. Other data presented in Muto, et al. (1989b) presented a displacement time history at the center of the panel from experimental observations. The maximum displacement during the experiment was about 12 cm [4.7 in]. Figure 2-12 shows a comparison of the displacement time history observed in the experiment (Muto, et al., 1989b) with that obtained in the numerical simulation. This figure shows that the maximum displacement is simulated quite well, despite a slight delay in developing the maximum displacement from the time of impact.

Another quantitative comparison was made for missile penetration depth. Measured crater depth was approximately 21 cm [8.3 in] (Muto, et al., 1989b). This value compares well with the numerical simulation result. The approximate average depth of penetration observed in the numerical simulation is 22 cm [8.7 in]. The crater predicted in the numerical simulation is shown in Figure 2-13.

2.2.3 Summary of Parameter Estimation Analyses

The input parameters needed in the concrete damage model in the LS-DYNA computer code have been verified for a range of applications, as discussed in this chapter. Numerical

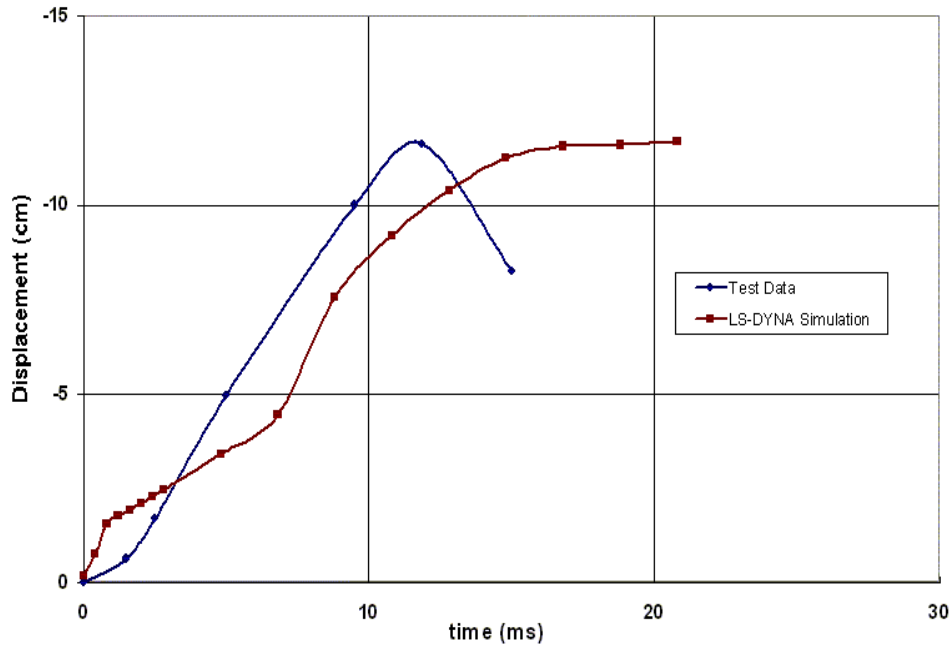

Figure 2-12. Displacement Versus Time Comparison For Full-Scale Idealized Jet Engine Experiment

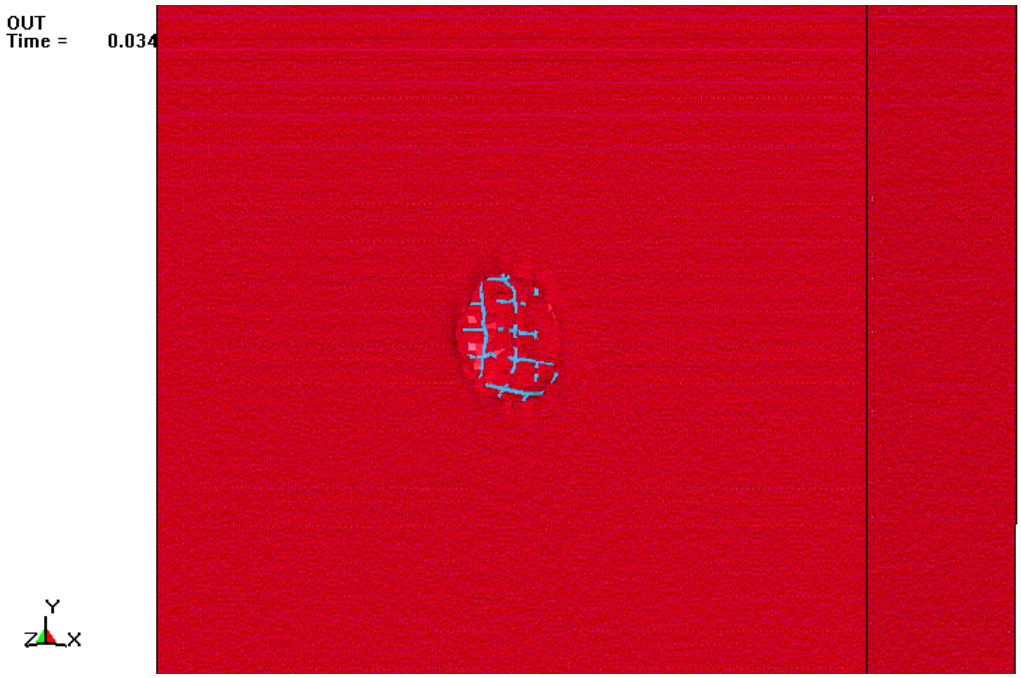

Figure 2-13. Crater on the Strike Face as Observed in the Simulation of Impact by a Full-Scale Idealized Jet Engine Missile

simulations performed for blast loading and missiles impacting reinforced concrete walls have shown very good agreement with available experimental results (Malvar, et al., 1997; Muto, et al., 1989a,b; Esashi, et al., 1989). These agreements between the LS-DYNA numerical simulations and experimental results give confidence that the material parameters needed for the concrete damage model

have been selected appropriately. These investigations are on going, and a study of the effects of hour glassing in the solid element used to model the concrete is in progress. Hour glassing is a term for nonphysical zero energy deformation modes in a solid element, and it can contribute to total system energy. The influence of hour glassing on the results will be quantified, and if necessary, controls will be used to limit its contribution to total system energy as it can never be eliminated completely in a solid element with single point integration.

3 PRELIMINARY IMPACT STUDY OF A HYPOTHETICAL STRUCTURE

A preliminary numerical simulation has been completed for one wall of a hypothetical structure. The wall was modeled as 47.9-m [157-ft] long, 19.5-m [64-ft] high, and 1.4-m [4.5-ft] thick section made of reinforced concrete. Additional interior intersecting walls were also included in the model. Damage of the concrete wall when impacted was modeled using the concrete damage model in LS-DYNA (Livermore Software Technology Corporation, 2003). The concrete has a compressive strength of 34.5 MPa [5,000 psi]. From the compressive strength, all additional input parameters were calculated, as described in Section 2 in the Appendix of this report. The wall is reinforced with #9 horizontal and #11 vertical steel reinforcement bars center to center at a spacing of 300 mm [12 in] with 150-mm [6-in] thick concrete cover from the surface of the wall to the edge of the bar. The compressive strength of the reinforcement bars used as reinforcement is assumed to be 414 MPa [60 ksi] with a yield strain of 0.002 and failure strain of 12 percent.

The steel is modeled with the plastic-kinematic material model in LS-DYNA (Livermore Software Technology Corporation, 2003). Failure criteria for the concrete elements were applied using a strain erosion algorithm available in LS-DYNA (Livermore Software Technology Corporation, 2003). A fixed boundary condition has been applied in the direction of loading for the top and bottom of the wall. Interior intersecting walls also are restrained in the direction of loading. Two views of the complete model showing the wall strike and rear faces are given in Figure 3-1.

An F-16 aircraft is assumed to impact the wall at a speed of 113 m/s [37 ft/s]. The time varying load, as provided by Hossain, et al. (1997), was determined using the Riera method (Riera, 1968). Loading was applied at the center of the wall over an area with 1.35 m [53 in] diameter according to the load curve presented in Figure 3-2. The loaded area of the model includes 225 nodes; therefore, the load has been divided by 225 and applied equally at each node.

Results from the numerical simulation show a maximum displacement of about 76 mm [3 in] at the center of the wall. This is shown as a displacement time history of a node located on the backside of the wall at the center of the impact area in Figure 3-3. Results of the numerical simulation also indicate tensile failure occurring at the backside of the wall. This is evident from contours of stress at the rear side of the wall at peak deflection and indicate that cracking is likely to occur somewhere within the regions of zero stress indicated in Figure 3-4.

Scabbing/spalling on the rear side of the wall was not evident in the numerical simulation. This was derived from the observation that no elements were eroded (i.e., deleted) in the numerical simulation by the strain erosion algorithm.

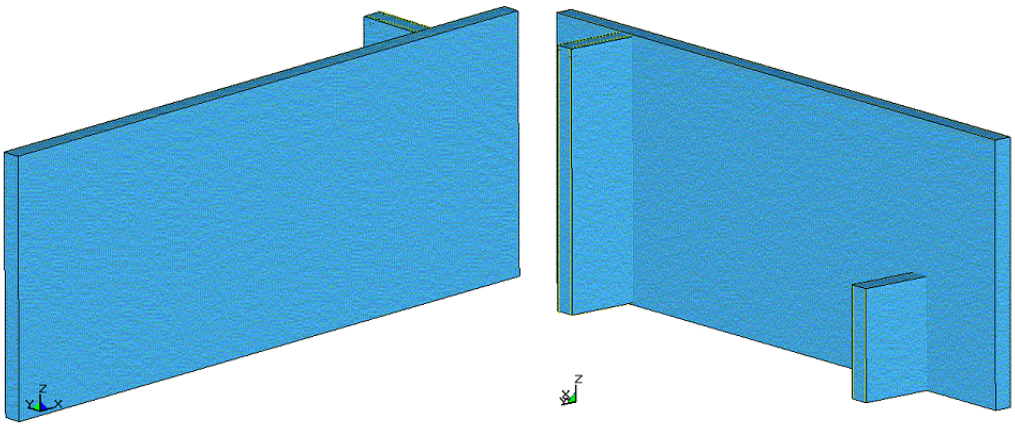

Figure 3-1. LS-DYNA Model of a Wall of a Hypothetical Structure. Both Front (Left) and Back (Right) Views Are Shown.

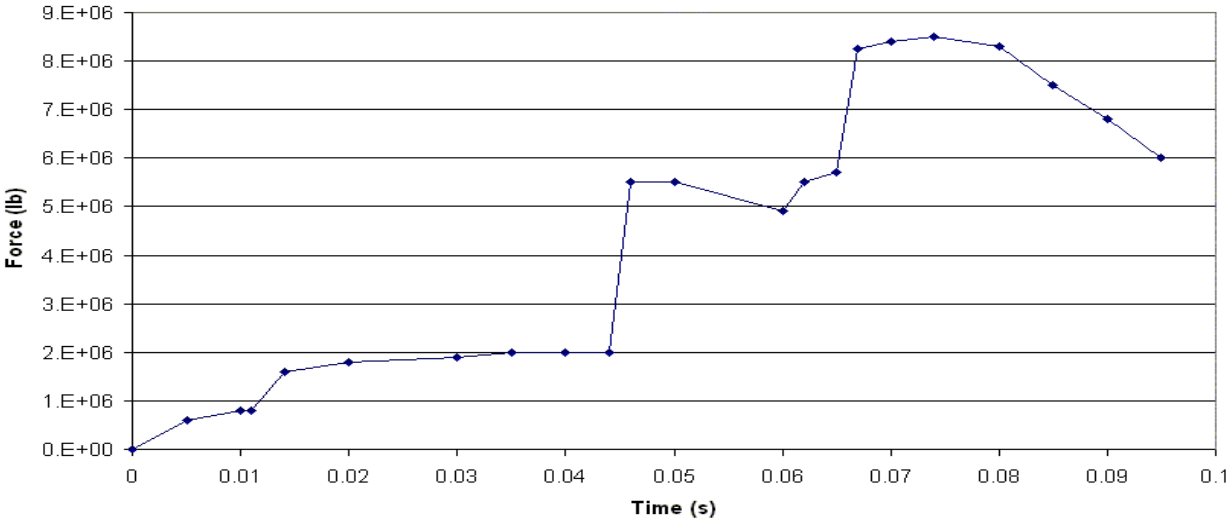

Figure 3-2. Force-Time History of Aircraft Impact From Hossain, et al. (1997) [1 lb = 0.454 kg]

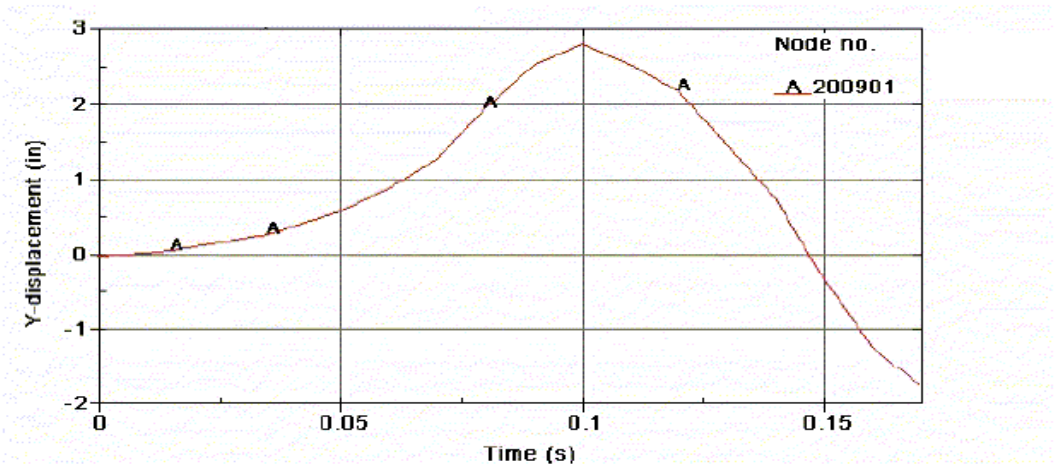

Figure 3-3. Displacement of the Wall Versus Time for an Impact of an F-16 at a Speed of 113 m/s [371 ft/s]

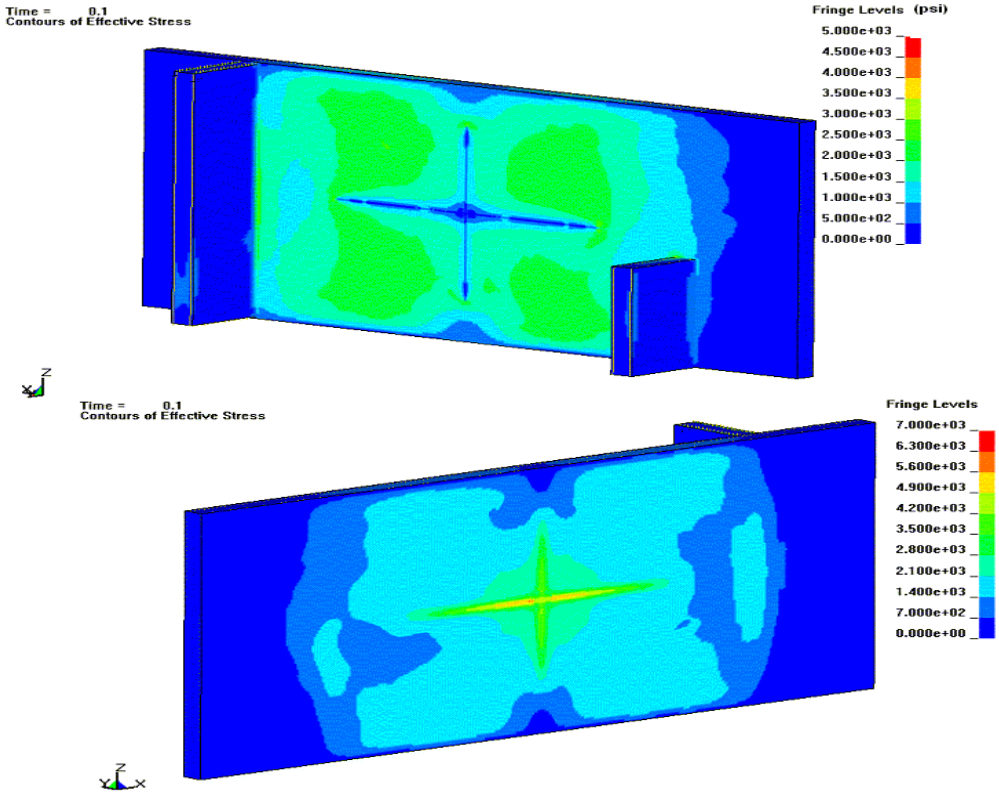

Figure 3-4. Contours of Effective Stress on the Rear (Top) and Strike Face (Bottom) of the Wall in a Hypothetical Structure

4 SUMMARY AND CONCLUSIONS

Experiments to investigate blast and missile impact damage to reinforced concrete walls have been simulated using the computer code LS-DYNA Version 970, and the numerical simulation results have been compared with published results. The comparisons have shown good correlation between measurements and calculated results. The good correlation indicates that the methodology, including how the material is characterized, is able to appropriately model such events. Analyzing problems that involve both blast and impact loads increases confidence that the selected methodology is robust.

In addition to numerical simulations of experiments, impact on a hypothetical reinforced concrete wall by an aircraft was modeled. The model, created to study local damage from aircraft impact, rather than overall building response, included a large expanse of wall with limited internal supporting components. Localized loads to simulate aircraft impact were taken from a published study and applied to the wall. The modeling approach, patterned after that shown to work well in the numerical simulations of experiments, also appeared to give reasonable results for the facility wall. This was only an experiment case. Actual facility structures will be modeled as details are made available and the threats (e.g., aircraft, impact velocities, and impact locations) are better defined under safeguard restrictions.

The overall conclusion from this study is that the methodology and material characterization parameters selected provide a good match to experimental results for problems that are similar to those that will be encountered in actual aircraft crash analysis to be conducted as the continuation of the present study.

5 FUTURE WORK

DOE (Ragan, 2005) has selected F-16s as the representative aircraft for estimating the annual frequency of military aircraft crashing onto the surface facilities of the potential repository because it has the highest crash rate. This might be acceptable if the estimated annual crash frequency was not reduced by taking credit for the robustness of certain structures or portions there of. In the analysis presented by Ragan (2005), estimated annual frequency has been reduced assuming walls of the waste handling buildings, barrier walls of the aging facility, and the transportation casks would be able to withstand a crashing F-16 aircraft at 95th percentile of the impact speed distribution. The basis of selecting F-16s as the representative aircraft, which has the potential of creating maximum damage to the structures, is not clear as there are other types of military aircraft flying in the immediate vicinity of the surface facilities (Ashley, 2005). These aircraft include F-15s and A-10s. Additionally, newer aircraft, such as F-22s, may also fly close to the surface facilities of the potential repository when deployed. These aircrafts have different weights due to differences in configuration. Consequently, the critical impact speed, that is, the impact speed at which the crashing aircraft will cause a breach of the structure, will be different.

It is not clear which aircraft DOE will select as the most critical from structural robustness assessment. The damage potential of a crashing aircraft depends on several factors and is defined as a combination of the mass of the aircraft (or any hard components, such as engine, landing gear, etc.) and the speed of the impact. Any of the aircraft types discussed above may have a potential to cause a breach of the structures beyond the critical speed. This speed should be different for each aircraft type due to difference in mass (more specifically, distribution of mass) along with available hard components.

Based on above discussion of the complexity of selecting the representative aircraft type for demonstrating structural robustness against accidental crashes, staff proposes to conduct independent studies on several aspects to develop capabilities to independently verify DOE assessments. The list of proposed activities is given below. It should be noted that the list is somewhat dependent on what DOE presents as its proposed approach.

- An assessment of the effect of hour-glassing on solid elements is currently in progress.

- Impact force-time histories for selected aircraft and engines (e.g., F-15, F-16, A-10, F-22 if information is available) will be developed using the Riera method (Riera, 1968, 1980). The force-time histories will be verified by comparing the time histories developed from experiment data (Muto, et al., 1989b). Additionally, information on the dimensions and weight of hard components of an aircraft will be collected to determine penetration capabilities.

- The force-time histories of the aircraft and the engine will be used to determine the global or overall response and local response or penetration of the walls of the waste handling facilities and the barrier walls of the aging facility.

- A parametric study will be conducted to determine the minimum thicknesses of concrete and steel members necessary to prevent a breach. This information will help determine whether the facility walls have sufficient thickness to preclude any local penetration by a crashing aircraft and associated hard components.

- Finite element models to determine global or overall response of the structure will be developed under impact from a crashing aircraft as opposed to localized damage to individual components. The force-time histories developed will be used in the calculation to independently verify the adequacy of the DOE assessment of the robustness of the walls of different structures.

- An analysis will be conducted to estimate the load-deformation characteristics of the walls filled with gravel under an impact load. Current understanding of the design of the aging facility barrier is that it will be made of two vertical walls spaced approximately 3.3 m [10 ft] apart and filled with gravel or crushed materials. The barrier may be made by joining segments of the walls.

6 REFERENCES

ANSYS, Inc. "ANSYS LS-DYNA." Version 9.0. Canonsburg, Pennsylvania: ANSYS, Inc. 2005.

Ashley, K.L. "Identification of Aircraft Hazards." 000–30R–WHS0–00100–000–005. Las Vegas, Nevada: Bechtel SAIC Company, LLC. 2005.

Brit, J., R. Robert, E. Dale, and C.E. Joachim. "Blast-X Code Version 4.2 User's Manual." U.S. Army Corps of Engineers. Engineering Research and Development Center, Geotechnical and Structures Laboratory. EDRC/GSL TR–01–2. 2001.

Esashi, Y., H. Ohnuma, C. Ito, and K. Shirai. "Experimental Studies on Local Damage of Reinforced Concrete Structures by the Impact of Deformable Missiles, Part 2: Intermediate-Scale Tests." Transaction of the 10th International Conference on Structural Mechanics in Reactor Technology (SMiRT 10). Los Angeles, California: American Association for Structural Mechanics in Nuclear Reactors. 1989.

Hossian, Q. A., R.P. Kennedy, R.C. Murray, K. Murteja, and B.P. Tripathi. "Structures, Systems, and Components Evaluation Technical Support Document, DOE Standard, Accident Analysis for Aircraft Crash into Hazardous Facilities." UCRL–ID–123577. 1997.

Hyde, D.W. "ConWep–Application of TM 5–855–1." Vicksburg, Mississippi: U.S. Army Engineer Waterways Experiment Station. 1992.

Hyde, D.W. "ConWep Version 2.1.0.0." Vicksburg, Mississippi: U.S. Army Engineer Waterways Experiment Station. 2004.

Livermore Software Technology Corporation. "LS-DYNA User's Manual." Version 970. Livermore, California: Livermore Software Technology Corporation. 2003.

Malvar, L.J., J.E. Crawford, J.W. Wesevich, and D. Simons. "A Plasticity Concrete Material Model for DYNA3D." *International Journal of Impact Engineering*. Vol 19, Nos. 9–10 pp. 847–873. 1997.

Muto, K., H. Tachikawa, T. Sugano, H. Tsubota, H. Kobayashi, Y. Kasai, N. Koshika, and T. Tsujimoto. "Experimental Studies on Local Damage of Reinforced Concrete Structures by the Impact of Deformable Missiles, Part 1: Outline of the Test Program and Small-Scale Tests." Transaction of the 10th International Conference on Structural Mechanics in Reactor Technology (SMiRT 10). Los Angeles, California: American Association for Structural Mechanics in Nuclear Reactors. August 14–19, 1989a.

Muto, K., H. Tachikawa, T. Sugano, H. Tsubota, N. Nagamatsu, N. Koshika, M. Okano, K. Suzuki, and S. Ohrui. "Experimental Studies on Local Damage of Reinforced Concrete Structures by the Impact of Deformable Missiles, Part 3: Full-Scale Tests." Transaction of the 10th International Conference on Structural Mechanics in Reactor Technology (SMiRT 10). Los Angeles, California: American Association for Structural Mechanics in Nuclear Reactors, August 14–19, 1989b.

Morissette, R.P. and J.A. Ziegler. "Identification of Aircraft Hazards." TDR–WHS–RL–000001, Revision 00. Las Vegas, Nevada: Bechtel SAIC Company, LLC. June 2002.

U.S. Nuclear Regulatory Commission. NUREG–1804, "Yucca Mountain Review Plan." Final Report. Washington, DC: NRC. 2003.

Ragan. G.E. "Frequency Analysis of Aircraft Hazards for License Application." 000–00C–WHS0–00200–000–00C. Las Vegas, Nevada: DOE, Office of Civilian Radioactive Waste Management. May 2005.

———. "Frequency Analysis of Aircraft Hazards for License Application." CAL–WHS–RL–000001. Rev. 00B. Las Vegas, Nevada: DOE, Office of Civilian Radioactive Waste Management. June 2003.

Reamer, C.W. and A.V. Gil. "Summary Highlights of NRC/DOE Technical Exchange and Management Meeting on Pre-Closure Safety." Las Vegas, Nevada: July 24–26, 2001.

Riera, J.D. "On the Stress Analysis of Structures Subjected to Aircraft Crash on Building Structures." *Nuclear Engineering and Design*. Vol. 8. pp. 415–426. 1968.

Riera, J.D. "A Critical Reappraisal of Nuclear Power Plant Safety Against Accidental Aircraft Impact." *Nuclear Engineering and Design*. Vol. 57. pp. 193–206. 1980.

Schlueter, J.R. "Comments Regarding Identification and Estimation of Aircraft Hazards for the License Application of the Proposed Repository at Yucca Mountain Related to Key Technical Issue (Kti) Agreement Preclosure 3.01." Letter from J.R. Schlueter to Joseph D. Ziegler, Acting Director, Office of License Application and Strategy, U.S. Department of Energy. NRC, Washington, DC: NRC. September 16, 2003a.

Schlueter, J.R. "Comments Regarding Frequency Analysis Hazards for License Application Report for the Proposed Repository at Yucca Mountain Related to Key Technical Issue (KTI) Agreement Preclosure 3.01." Letter from J.R. Schlueter to Joseph D. Ziegler, Acting Director, DOE, Office of License Application and Strategy, U.S. Department of Energy. NRC, Washington, DC: NRC. September 17, 2003b.

Wang, C.-K. and C.G. Salmon. "Reinforced Concrete Design." 6th Edition. Reading, Massachusetts: Addison Wesley Educational Publishers, Inc. 1998.

APPENDIX

APPENDIX: DESCRIPTION OF LS-DYNA CONCRETE DAMAGE MATERIAL MODEL PARAMETERS

The concrete damage model is an improved version of the pseudo tensor model in LS-DYNA (Livermore Software Technology Corporation, 2003). This model offers a three-invariant stress versus pressure function description, which enables calculation of the yield function of the material. The initial yield function is developed by a combination of three fixed three-parameter functions of pressure. Volumetric response is prescribed in the form of a tabulated compaction curve, which describes the relation between the hydrostatic pressure and volumetric strain.

In the concrete damage model, after the initial yield strength is reached, the modified yield strength σ is described by

$$\sigma = \eta\left(\sigma_{\text{max}} - \sigma_{\text{yield}}\right) + \sigma_{\text{yield}} \tag{A–1}$$

σ_{max} and σ_{yield} are defined in Eq. (A–3)

A damage function $\eta(\lambda)$ is a user input and describes how the yield stress factor, η, varies with the modified effective plastic strain, λ. The function begins with the plastic strain equal to zero, increases to a value of 1 at some maximum effective plastic strain, then decreases to a value of zero at larger values of plastic strain. The values for this function were suggested by the LS-DYNA User's Manual (Livermore Software Technology Corporation, 2003) and used in this study. If the maximum strength is reached, a new yield strength is interpolated from the maximum and residual strengths using the following equation:

$$\sigma = \eta\left(\sigma_{\text{max}} - \sigma_{\text{residual}}\right) + \sigma_{\text{residual}} \tag{A–2}$$

A total of eight parameters describe the initial (concrete strength) as shown in Figure A–1. The equations describing the strength maximum σ_{max}, residual σ_{residual}, and yield σ_{yield} strengths are:

$$\sigma_{\text{max}} = a_o + \frac{p}{a_2 p} \tag{A–3}$$

$$\sigma_{\text{residual}} = \frac{p}{\left(a_{1f} + a_{2f} p\right)} \tag{A–4}$$

$$\sigma_{\text{yield}} = a_{0y} + \frac{p}{\left(a_{1y} + a_{2y} p\right)} \tag{A–5}$$

where,

p is pressure and other parameters are defined in Table A–1.

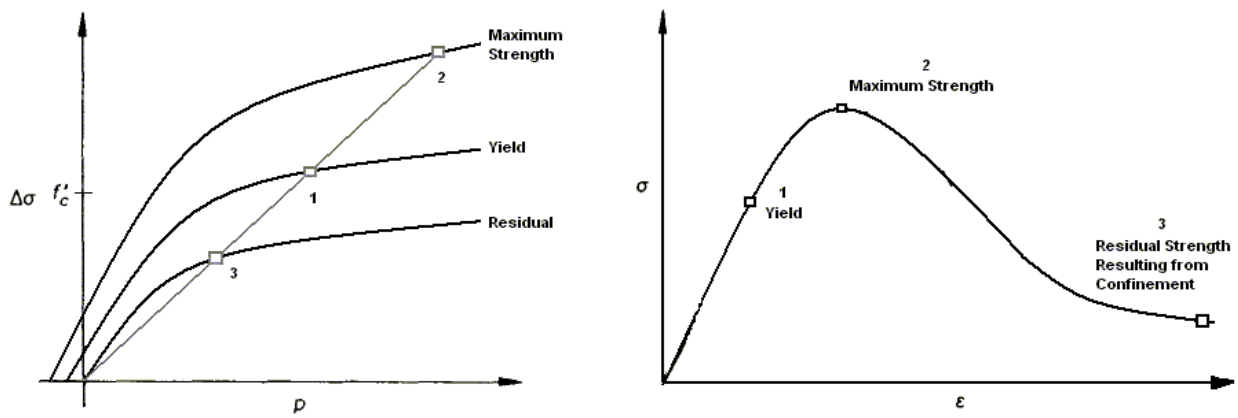

Figure A–1. Failure Surface Description in Concrete Damage Model (Malvar, et al., 1997)

The parameter a_0 represents the maximum failure strength at p = 0. This is estimated as $f_c' / 4$ where $f_c' / 4$ is the compressive strength of concrete. Parameter a_1 is estimated to be 1/3, and parameter a_2 is taken as $1/3 f_c'$. These values are taken directly from the LS-DYNA User's Manual (Livermore Software Technology Corporation, 2003). In addition, the initial yield strength is estimated by the following equation:

$$\sigma_y = 0.45 \left(a_0 + \frac{P}{a_1 + a_{2p}} \right) \qquad \text{(A–6)}$$

Parameters that describe the initial yield strength (a_{0y},a_{1y}, a_{2y}) are then adjusted so that a curve is generated, providing a match to that of Eq. (A–6).

Table A–1 gives a complete list of input parameters utilized in this study for the concrete damage model, along with their descriptions from the LS-DYNA User's Manual (Livermore Software Technology Corporation, 2003).

The pressure-compaction curve representing the volumetric response of the concrete is modeled using the tabulated compaction equation of state model in LS-DYNA. The data for the equation of state model was obtained by referring to the Winfrith Concrete Model in the LS-DYNA keyword user's manual (Livermore Software Technology Corporation, 2003). The manual suggests that in the event a pressure-compaction response curve specific to the concrete being modeled cannot be obtained from experimental data, a compaction curve can be specified using the following method.

For the tabulated model, pressure is defined as positive in compression, and volumetric strain is defined as the natural log of the relative volume, which is negative in compression. The recommended values of the response curve are shown in Table A–2.

Table A–1. List of Concrete Damage Input Parameters from LS-DYNA User's Manual*	
Parameter†	**Description**
MID	Material Identification
RO (ρ)	Mass Density
PR (ν)	Poisson's Ratio
SIGF (f_c')	Maximum Principal Stress for Failure
A0 (a_o)	Cohesion
A1 (a_1)	Pressure Hardening Coefficient
A2 (a_2)	Pressure Hardening Coefficient
A0Y (a_{0y})	Cohesion for Yield
A1Y (a_{1y})	Pressure Hardening Coefficient for Yield Limit
A2Y (a_{2y})	Pressure Hardening Coefficient for Yield Limit
A1F (a_{1f})	Pressure Hardening Coefficient for Failed Material
A2F (a_{2f})	Pressure Hardening Coefficient for Failed Material
B1 (b_1)	Damage Scaling Factor
B2 (b_2)	Damage Scaling Factor for Uniaxial Tensile Path
B3 (b_3)	Damage Scaling Factor for Triaxial Tensile Path
$\lambda_1 - \lambda_{13}$	Tabulated Damage Function
$\eta_1 - \eta_3$	Tabulated Scale Factor

*Livermore Software Technology Corporation. "LS-DYNA User's Manual." Version 970. Livermore, California: Livermore Software Technology Corporation. 2003.
†Parameters in capital letters are from the LS-DYNA input description. Corresponding parameters used in the equations of this Appendix are given in parenthesis.

Table A–2. Volumetric Strain Versus Tabulated Pressure	
Volumetric Strain	**Pressure (MPa)**
$-p_1/k$	$1.00 \times p_1$
−0.002	$1.50 \times p_1$
−0.004	$3.00 \times p_1$
−0.010	$4.80 \times p_1$
−0.020	$6.00 \times p_1$
−0.030	$7.50 \times p_1$
−0.041	$9.45 \times p_1$
−0.051	$11.55 \times p_1$
−0.062	$14.25 \times p_1$
−0.094	$25.05 \times p_1$

The parameters p_1 and K are calculated as follows:

$$p_1 = \frac{f_c}{3}$$
$$K = \frac{E_s}{3(1-2\nu)} \qquad \text{(A–7)}$$

where E_s is equal to one-half the tangent modulus of the concrete, ν is the Poisson's ratio for concrete, and f_c is the concrete unconfined compressive strength.

A full description of the concrete damage model can be found in Malvar, et al. (1997). Additionally, the LS-DYNA User's Manual (Livermore Software Technology Corporation, 2003) suggests tabulated values for the damage function to use with the concrete damage model, as given in Table A–3.

Erosion Algorithm

To complement the concrete damage model, an erosion algorithm was implemented to simulate concrete breakup. This erosion feature was used primarily as a visual and qualitative representation of concrete scabbing and spalling effects and was implemented using the MAT_ADD_EROSION feature, as found in the LS-DYNA User's Manual (Livermore Software Technology Corporation, 2003). This feature enables elements reaching a user-selected strain threshold to be deleted from calculation. Through a parametric study, which consisted of running numerical simulations with different erosion strain values and observing overall damage, an erosion strain parameter of 0.5 was selected. Using this value provided good overall results when compared with the experimental results, as demonstrated in Chapter 2.0 of this report.

Table 3. Tabulated Concrete Damage Function*	
Damage Function η(λ)	**Effective Plastic Strain λ**
0.309	0
0.543	8.62×10^{-6}
0.84	2.15×10^{-5}
0.975	3.14×10^{-5}
1	3.95×10^{-4}
0.79	5.17×10^{-4}
0.63	6.38×10^{-4}
0.469	7.98×10^{-4}
0.383	9.67×10^{-4}
0.247	1.41×10^{-3}
0.173	1.97×10^{-3}
0.136	2.59×10^{-3}
0	0.909

*Livermore Software Technology Corporation. "LS-DYNA User's Manual." Version 970. Livermore, California: Livermore Software Technology Corporation. 2003.

Additionally, a pressure erosion threshold, designed to limit the tensile pressure within an element, also was investigated. Numerical simulations were performed using a threshold value equal to 10 percent of the concrete compressive strength, a value somewhat higher than the true tensile strength of the concrete. In these numerical simulations, the pressure erosion algorithm identified the elements experiencing tension on the rear side of the wall and these elements were deleted, producing rather large gaps in the wall where normally small tensile cracks would be expected. With very fine grid resolution, this behavior may give a good approximation of tensile crack formation; however, for the mesh size that must be utilized in these types of problems, it is likely to over predict damage from tensile cracking. Early deletion of elements associated with the pressure erosion algorithm eliminates the element entirely from calculation, whereas cracked concrete elements still have mass and retain some residual strength in compression, shear, and even in tension in certain directions. It was, therefore, concluded that the pressure erosion algorithm was not well suited for these types of impact problems. It should be noted that the concrete damage model does account for a reduction in element strength when the tensile cut-off pressure is reached; however, the element is retained and still contributes to the strength and inertia of the wall. This formulation was used in this study.

REFERENCES

Livermore Software Technology Corporation. "LS-DYNA User's Manual." Version 970. Livermore, California: Livermore Software Technology Corporation. 2003.

Malvar, L.J., J.E. Crawford, J.W. Wesevich, and D. Simons. "A Plasticity Concrete Material Model for DYNA3D." *International Journal of Impact Engineering*. Vol 19, Nos. 9–10 pp. 847–873. 1997.